J Mater Sci (2007) 42:8083–8087
DOI 10.1007/s10853-007-1664-0

Morphological, structural and optical characterization of nickel nanostructures fabricated through electrochemical template synthesis

Raminder Kaur · N. K. Verma · S. K. Chakarvarti

Received: 11 December 2006 / Accepted: 5 March 2007 / Published online: 22 June 2007

Abstract The electrochemical template synthesis of high aspect-ratio nickel nanorods in the track-etch membranes of polycarbonate having nominal pore size of 80, 50 and 30 nm is considered. The morphological and structural analyses have been carried out through scanning electron microscopy and X-ray diffraction respectively. The synthesized nanorods possess FCC lattice structure with texturing for {220} planes. When excited with UV radiation pulse, the structures exhibited weak photoluminescence with exponential decay, which is attributed to the presence of some adsorbed metal hydroxide.

Introduction

Owing to the prospective applications of nanometer-sized materials in the fields of electronic and optical devices, there has been a significant research activity aimed at understanding the behaviour and properties of such nanostructures, as well as on developing techniques for controlling their properties. The physical and chemical properties in the nanostructured phase usually differ from those of bulk material due to the high surface area to volume ratio [1].

It is well known that the electrodeposited nickel exhibits texturing, resulting from a number competing processes, such as internal stresses of the deposits, growth of competing crystal faces, surface energies and selective inhibition of lattice growth due to adsorbed hydrogen. All these factors in turn are functions of various parameters such as current density, pH value of the bath, electrolyte concentration and type of additives used and their concentration. In addition, as both copper and nickel have a FCC lattice structure with very close lattice constants of 0.361 and 0.352 nm respectively, the copper substrate will introduce its statistically orientated texture into the first seeds of the electroplated nickel.

R. Kaur (✉) · N. K. Verma
Thapar Institute of Engineering & Technology, Patiala, Punjab 147001, India
e-mail: raminder_k_saini@yahoo.com

S. K. Chakarvarti
National Institute of Technology, Kurukshetra 136119, India

Fabrication and morphological characterization

In the present work, the technique of template synthesis has been employed for fabricating high aspect-ratio nanowires of nickel. For template synthesis, the nuclear track filters (NTFs) of polycarbonate membrane were obtained from M/s Nuclepore Corporation, UK. These NTFs had nominal pore size of 80, 50 and 30 nm, with a pore density of 10^8 cm^{-2} and 10 μm thickness. The electrodeposition of nickel metal takes place through the pores, whose dimensions and geometry, therefore, dictate the morphology and geometry of the nascent microstructures thus produced.

Two-electrode electrochemical cell has been used for nickel deposition in the pores of the template. Similar cell design has been used previously for fabricating copper microstructures [2]. The cell was filled with freshly prepared and filtered electrolyte, i.e., 2.28 N (45 g/150 ml) $NiSO_4 \cdot 6H_2O$ dissolved in double-distilled, de-ionized water at room temperature (35 °C). Nickel chloride was not added to the electrolyte as it causes internal stresses in the deposits, which could lead to uprooting of the high aspect-ratio nanowires from the substrate. 30 g/l of boric acid was

added to the electrolyte to act as buffering agent and stabilize the pH in the cathode film. It has the advantages of low cost and availability in purified form [3]. The pH of the solution measured 2.14.

The cathode efficiency becomes a very important parameter during template synthesis. In ordinary industrial electroplating process, a cathode efficiency of around 92 to 97% would be considered as acceptable. However, in case of template synthesis of high aspect-ratio nanowires of very small diameters, any evolution of hydrogen will form a non-conducting bubble, which will get stuck within the pores of the template and cannot be removed by processes such as agitation of bath. However, very small amounts of hydrogen may get co-deposited along with nickel through adsorption, without making the pores non-conductive. This co-deposited hydrogen does influence the texture of the resulting nanostructures through differential inhibition of different (*hkl*) planes [4]. Thus, it is possible to exercise control on texture formation through plating parameters.

The electrodepositions were performed potentiostatically at room temperature (35 °C) and a low current density of 6 mA/cm^2 was found to yield good results by avoiding side reactions such as hydrogen evolution.

After the deposition, the polycarbonate templates with nickel nanostructures were immediately removed from the electrolyte, first rinsed with double-distilled water and ethanol and then dried in air at room temperature. The porous polycarbonate membrane was removed by dissolving it in dichloromethane for 10 min, thereby leaving behind the nanostructures on the copper cathode substrate. Keeping in view the fragility of these high aspect ratio nanostructures, the specimens were not washed with distilled water, as the hydrodynamic pressure, coupled with high surface tension of water is likely to remove the nanostructures from the substrate.

The cleaned and dried samples, were mounting on specially designed aluminium stubs with the help of double-sided adhesive tape and viewed under ''Joel, JSM 6100 Scanning Electron Microscope'' at an accelerating voltage of 20 kV. It may be mentioned that as the specimens were to be subsequently analyzed for optical characteristics, they were not coated with a layer of gold palladium alloy for contrast enhancement. Images of these ''raw'' specimens were recorded on the photographic film in the form of negatives at different magnifications. Figure 1 shows SEM of the microstructures formed. The micrograph reveals that the nanostructures are very fragile and easily damaged by hydrodynamic forces during membrane dissolution.

Structural characterization

In order to confirm the crystalline quality of the deposits, fresh synthesis was carried out and in this case, the membrane containing nascent microstructures was peeled-off from the copper substrate and X-ray diffraction of the deposited microstructures was carried out using D/Max Rint 2000 Rigaku (Tokyo) X-ray diffraction machine using characteristic copper Kα wavelength of 1.5418 Å.

The three peaks have been obtained in the X-ray scan (refer Fig. 2), in the 2θ span ranging from 40° to 80°. Applying extinction rules, these peaks and associated *d*-values have been found to correspond to the nickel *hkl* planes (111), (200) and (220) as given in Table 1, thus confirming FCC structure of the microstructures formed.

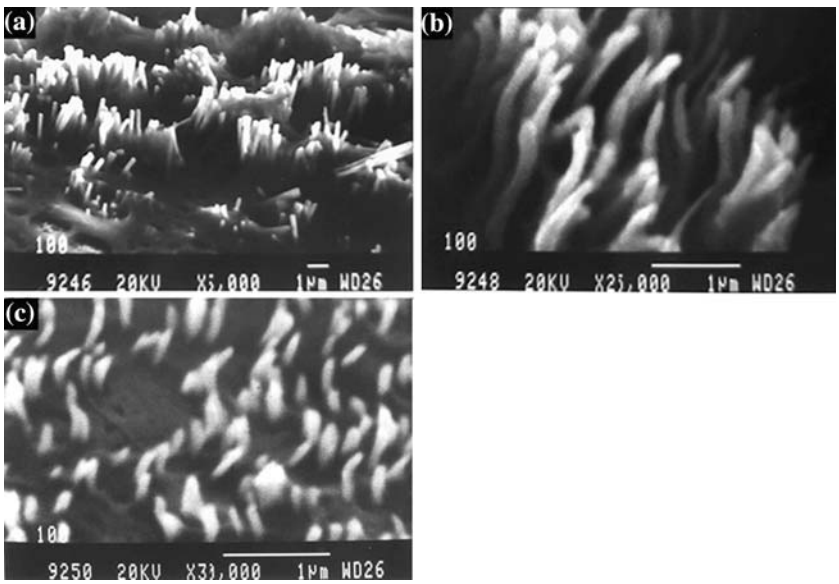

Fig. 1 Scanning electron micrographs showing (**a**) 80 nm, (**b**) 50 nm and (**c**) 30 nm diameter nickel microstructures

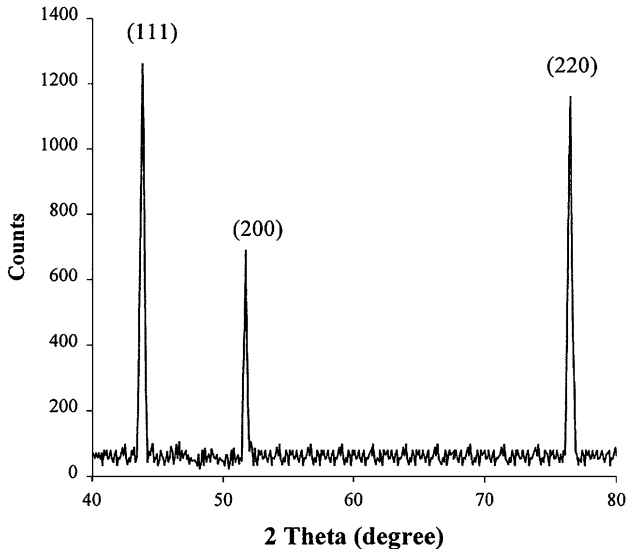

Fig. 2 X-Ray diffractogram for 80 nm Ni microstructures

A comparison of observed peak intensity with random nickel specimen has been carried out using the Harris relationship [5] as given below:

$$P(h_i k_i l_i) = \frac{I(h_i k_i l_i)}{I_0(h_i k_i l_i)} \left[\frac{1}{n} \sum_{i=1}^{n} \frac{I(h_i k_i l_i)}{I_0(h_i k_i l_i)} \right]^{-1}$$

where $P(hkl)$ is the texture coefficient of the plane specified by Miller Indices (hkl); while $I(hkl)$ and $I_0(hkl)$ are the specimen and standard intensities respectively for a given peak, and n refers to the total number of diffraction peaks considered. The analysis (Refer Table 2) reveals a strong texturing for {220} planes. This result is in accordance with the general observation for additive-free Watts baths having pH < 2.5, which are known to yield textures along ⟨110⟩, ⟨100⟩ or ⟨210⟩ lattice directions [6].

Optical characterization

In order to investigate the effect of confinement on the fabricated Ni nanostructures in relation to photoluminescence, the fabricated structures, after morphological characterization, were placed at an angle of 45° in front of the ultraviolet laser radiation pulse from a nitrogen laser

Table 1 Determination of lattice structure

2θ	Sin θ	Sin^2 θ	Ratios	Normalized Ratios	Lattice Planes
44.24	0.37	0.14	1.00	3	(111)
51.80	0.44	0.19	1.33	3.98 ≈ 4	(200)
76.03	0.62	0.38	2.66	7.99 ≈ 8	(220)

Table 2 Determination of texture coefficient of electrodeposited nickel

D values (Å)		hkl	Intensity		Texture Coefficient $P(hkl)$
Standard	Observed		Standard I_0	Observed I	
2.034	2.047	111	100	100	0.518
1.760	1.765	200	46	56	0.636
1.244	1.252	220	26	93	1.845

(10 kW, Ultraviolet) with a pulse duration of a 1–5 nanoseconds.

The phenomenon of photoluminescence is generally characterized by absorption of radiation of a particular energy, followed by the emission of radiation of lower energy. Accordingly, the radiation emitted by the specimen as a result of UV excitation was made to pass through a glass slab for absorbing any UV content, followed by its passage through a monochromator for selecting a particular range of wavelengths in the signal being recorded. The emission from the UV excited microstructures was collected by a fast photomultiplier tube having a rise time of a 1–5 nanoseconds. The signal from photomultiplier tube was fed to a storage type oscilloscope, from where the data was transferred to a PC for subsequent analysis. The detailed description of the experimental set-up used for recording optical spectra is given in Fig. 3.

The decay curve obtained for 400 nm output emission wavelength from 80 nm microstructures is shown in Fig. 4. The decay obeys exponential rule with a decay constant of 0.18, which corresponds to a decay time of 5.49 μs.

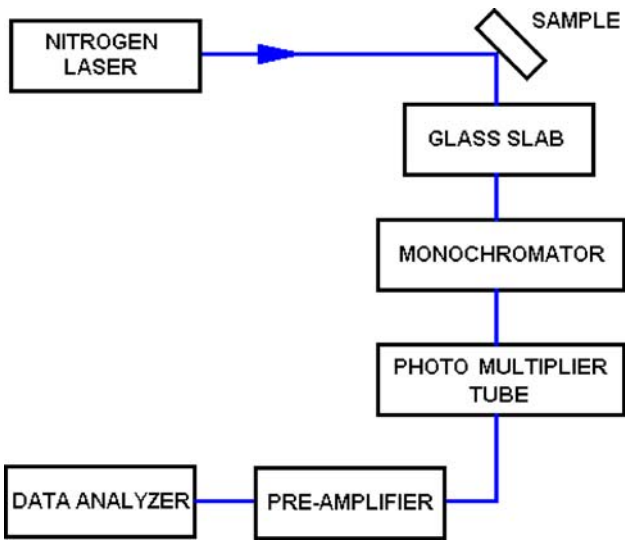

Fig. 3 Block diagram of experimental set-up for recording photoluminescence spectra

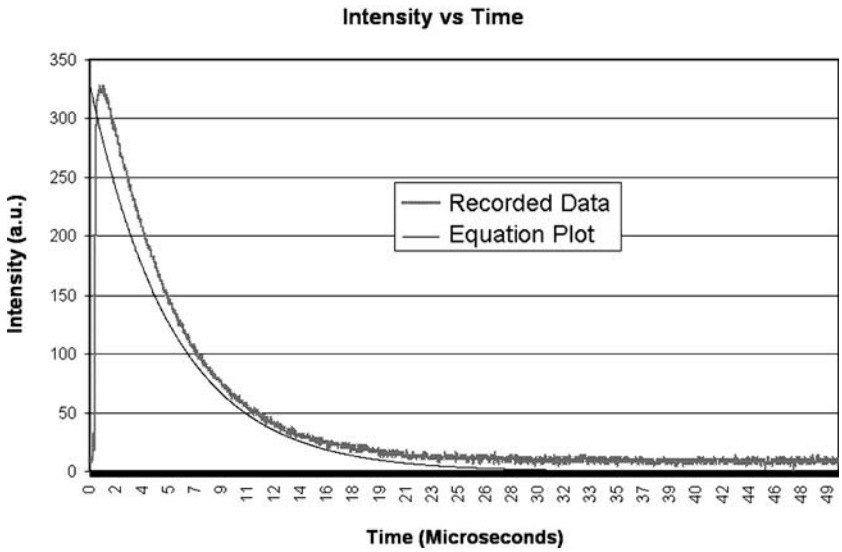

Fig. 4 Photoluminescence decay curve at 400 nm wavelength for 80 nm Nickel nanostructures

Table 3 Decay times for various specimens at different emission wavelengths

S. No.	Sample	Decay Time (μs) at various emission wavelengths (nm)						
		400	450	500	550	600	650	700
1	Nickel, 80 nm	5.49	5.11	4.98	5.14	5.17	5.27	5.02
2	Nickel, 50 nm	5.26	5.27	5.27	5.44	5.27	5.97	4.90
3	Nickel, 30 nm	5.15	5.59	6.14	5.18	5.28	5.83	5.72
4	Nickel Anode	–	–	–	–	–	–	–
5	$NiSO_4 \cdot 6H_2O$	5.17	5.37	4.77	5.00	5.43	5.91	4.96
6	Polycarbonate	4.69	5.81	5.89	5.81	5.64	5.26	5.62

In order to account for the possible causes of this unexpected emission, it was thought that the emissions were caused due to some contaminants, viz. impurities in the nickel metal, leftover electrolyte or remnants of polycarbonate template. Therefore, comprehensive photoluminescence tests were conducted on various materials at different emission frequencies, as detailed in Table 2. The nickel anode material did not give any emissions, thus ruling out the possibility of any impurities in the anode material. All other materials exhibited exponential decay with a similar decay constant of the order of 0.18 per second, corresponding to a decay time of around 5.5 μs (Table 3).

In addition to the decay time, the profiles of peak intensity obtained at various emission wavelengths were also plotted. These intensity profiles were found to be very characteristic of the given material, as can be seen from Fig. 5. Just as expected, the organic material of the polycarbonate membrane exhibited the brightest emissions, while the intensity of the two kinds of nickel nanostructures and nickel sulphate are somewhat comparable. However, the $NiSO_4 \cdot 6H_2O$ exhibits peak at 470 nm,

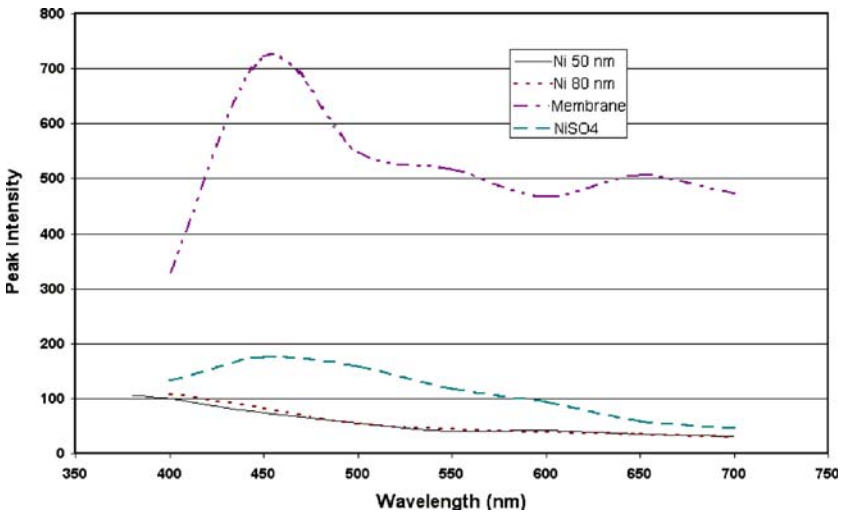

Fig. 5 Photoluminescence peak intensity for various emission wavelengths

which is in contrast to the nickel nanostructures. This once again eliminated the possibility of any contaminant playing role in the photoluminescence exhibited by nickel nanostructures.

So, the photoluminescence can be attributed to either of the two possibilities: First, the presence of some nickel hydroxide that might have got adsorbed during electrodeposition of the microstructures, or due to oxide formation on the surface layer owing to its large surface area to volume ratio. However, the formation of a similar oxide layer should also have caused the bulk anode to exhibit photoluminescence, which, it has been observed, does not yield any detectable emissions. Accordingly, the emissions may be attributed to some compound like nickel hydroxide, which might have got adsorbed at the time of electrodeposition as a result of local increases of pH in the Helmholtz double layer [7].

Conclusions

In conclusion, template synthesis is an elegant technique for preparing metallic nanostructures having high aspect ratios. The fabrication process is quite sensitive towards various parameters during electrodeposition, particularly cathode efficiency, as hydrogen bubbles tend to clog the pores. Electrolyte concentrations equivalent to Watts solution, except for $NiCl_2$ constituent lead to successful fabrication of nanostructures in the pores of 80, 50 and 30 nm diameters. The nanostructures are very fragile and easily damaged by hydrodynamic forces during membrane dissolution. X-ray diffractogram shows a FCC crystalline nature of the deposited nickel nanostructures with strong texturing for {220} planes. Photoluminescence studies reveal that the fabricated nanostructures exhibit some weak photoluminescence, which obeys exponential decay with a decay constant of around 0.18 s^{-1}. This strange behaviour is thought to be due to the presence of adsorbed hydroxides.

Acknowledgement We gratefully acknowledge the generous financial support provided by All India Council for Technical Education (AICTE), Govt. of India, New Delhi, for this research work, vide their letter number F/No/8020/RID/R&D-84-2001-02 dated March 4, 2002.

References

1. Reetz MT, Helbing W, Quaiser SA, Stimming U, Breuer N, Vogel R (1995) Science 267:367
2. Kaur R, Vema NK, Chakarvarti SK, Kumar S (2006) J Mater Sci 41:3723
3. Di Bari G (1994) ASM Metals Handbook: Surface Eng 5:201
4. Reddy A, Ragagopalan S (1963) J Electronal Chem 6:153
5. Barrett CS, Massalski TB (1980) Structure of Metals Oxford: *Pergamon* 204
6. Bergenstof Nielsen C, Horsewell A, Ostergard MJL (1997) J Appl Electrochem 27:839
7. Amblard J, Epelboin I, Froment M, Maurin G (1979) J Appl Electrochem 9:233